Supplement of Earth Syst. Dynam., 16, 1085–1102, 2025
https://doi.org/10.5194/esd-16-1085-2025-supplement

Supplement of

A causality-based method for multi-model comparison: application to relationships between atmospheric, oceanic and marine biogeochemical variables

Germain Bénard et al.

Correspondence to: Germain Bénard (germain.benard@lsce.ipsl.fr)

Contents

S1 Additional information on biogeochemical models

The marine biogeochemistry models used present similar complexity but still have different implementations. Table S1 displays the main components of these models, including the plankton functional types, the nutrients, as well as the organic detrital pool. Beyond these structural differences, these models also differ

Model	Elements						Detrital organic fraction	Biology		Reference
	N	P	Si	Fe	C	O_2		Phytoplankto	Zooplankto	
PISCES-v2 (IPSL-CM6A-LR)	✓	✓	✓	✓	✓	✓	3 cat.	Diatoms, Nanophyto.	Microzoo., Mesozoo.	Aumont et al. (2015)
BFM5.2 (CMCC-ESM2)	✓	✓	✓	✓	✓	✓	3 cat.	Diatoms, Nanophyto.	Microzoo., Mesozoo.	Vichi et al. (2015); Lovato et al. (2022)
MARBL (CESM2)	✓	✓	✓	✓	✓	✓	6 cat.	Diatoms, Diazotrophs, Nano/picophyto.	Zoo.	Long et al. (2021)
CanOE (CanESM5-CanOE)	✓			✓	✓	✓	2 cat.	Large phyto., Small phyto.	Large zoo., Small zoo.	Christian et al. (2021)
MEDUSA-2.0 (UKESM1-0-LL)	✓		✓	✓	✓	✓	2 cat.	Diatoms, Picophyto.	Microzoo., Mesozoo.	Yool et al. (2013)
OECO2 (MIROC-ES2L)	✓	✓		✓	✓	✓	1 cat. (Flux Attenuation)	Non-diazotroph phyto., Diazotrophs	Zoo.	Hajima et al. (2020); Séférian et al. (2020)

Table S1: Table detailing for each biogeochemical model the nutrients, detrital organic fractions, and plankton functional types modelled

in their parameterizations. The biogeochemical cycles, although representing the same fundamental processes, may differ in their mathematical implementation. Nutrient sources vary between models, as do the equations governing biological processes and the sedimentation of organic matter. Séférian et al. (2020) presents in its second table a detailed overview of the different external nutrient sources implemented in biogeochemical models. The CMCC-ESM2 model may be missing from this research, yet we can still observe the substantial variations in our model selection. The UKESM1-0-LL model is distinguished by the absence of external nutrient sources. In contrast, CanESM5-CanOE integrates inputs via sediments and atmospheric deposition, but only for iron. The IPSL-CM6A-LR and CESM2 models present a greater diversity of sources, including not only atmospheric deposition but also riverine inputs for nitrogen, phosphorus, and iron. Moreover, in these latter two models, atmospheric deposition contributes to nitrogen input, and in the specific case of CESM2, silica and phosphorus as well. The MIROC-ES2L model with OECO2 incorporates iron input from sediments, iron and nitrogen from atmospheric deposition, and nitrogen and phosphorus from riverine sources. Regarding CMCC-ESM2, Lovato and Butenschön (2020) indicates that this model incorporates riverine inputs for phosphorus, nitrogen, and iron, as well as atmospheric deposition for iron.

S2 Supplementary Figures

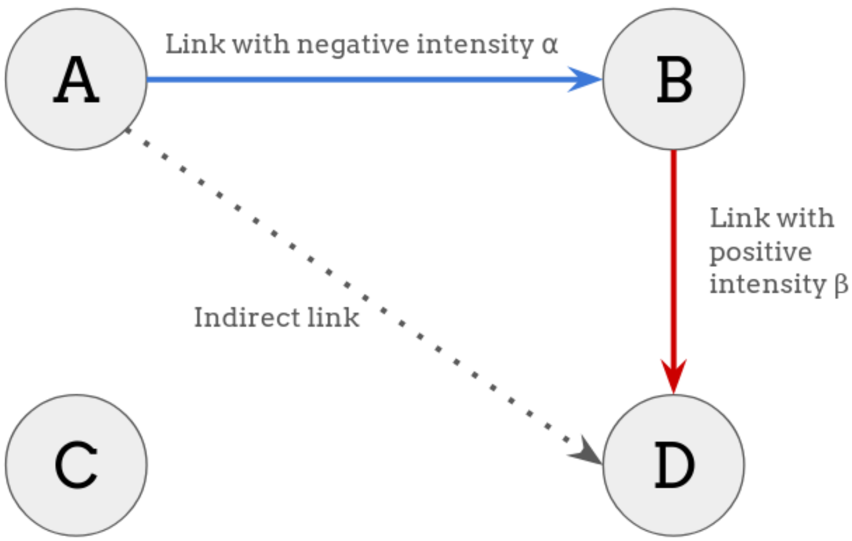

Figure S1: Example of causal graph. Edges (colored arrows) correspond to a causality link with an intensity and a potential lag. The intensity can be positive (red) or negative (blue). In the main article, the nodes (A,B,C and D) correspond to oceanic, atmospheric and biogeochemical variables. This conceptual example shows direct links between A and B, and between B and D. While there is no direct link between A and D in the causal graph, A influences D indirectly through B. Some variables can be isolated from others with no causal links. In this example, C is isolated from the other variables."

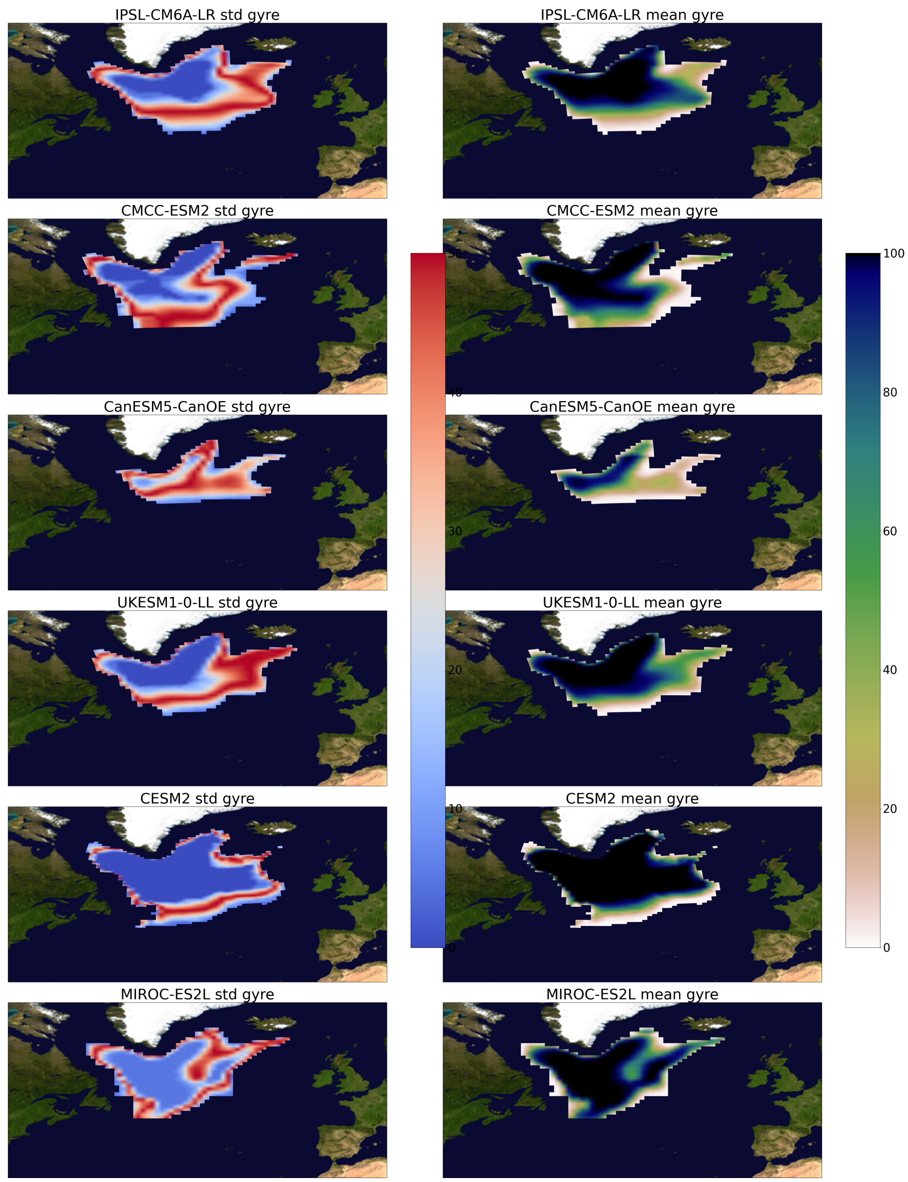

Figure S2: The subpolar gyre and its variability among the 5 Earth System models. Left column: "std gyre" indicating variability expressed by the standard deviation of appearance. The points in red are the points varying the most. Right column: the"mean gyre" metrics indicating, in percentage, how often each point is considered as part of the gyre. A grid point having 100% indicates that for each time step this point is part of the gyre. *Map credit: NASA-Visible Earth: The Blue Marble Land Surface, Ocean Color and Sea Ice*

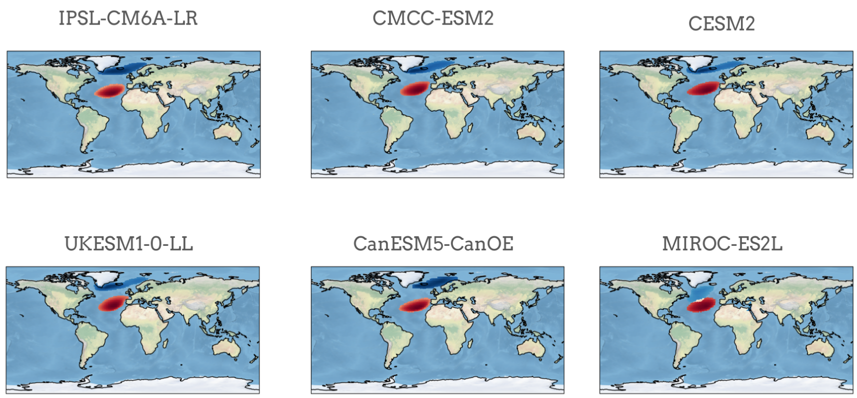

Figure S3: Sea Level Pressure poles used for the computation of the North Atlantic Oscillation index. In red the high pressure pole and in blue the low pressure one.

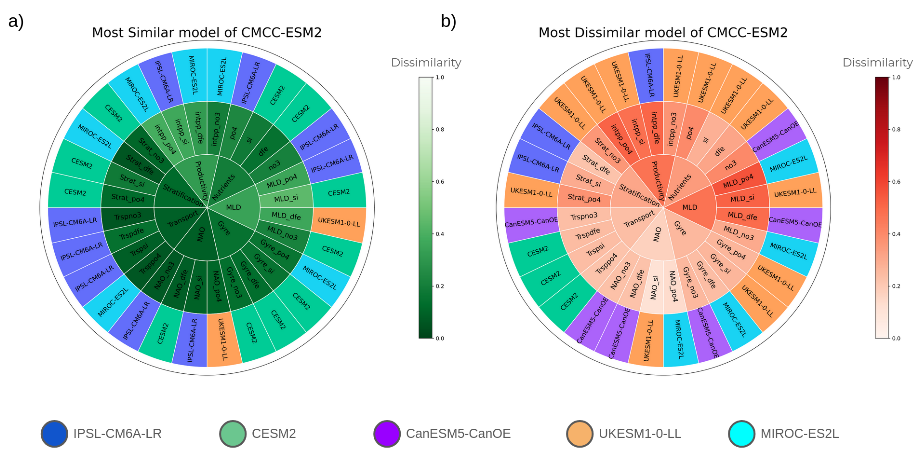

Figure S4: Most similar (a) and dissimilar (b) models compared to CMCC-ESM2 based on the dissimilarity metric in Eq.2. The inner circle indicates the variable, the middle circle shows each variable's variant depending on which nutrient is considered("_no3" for nitrate,"_dfe" for dissolved iron, "_si" for silicate and "_po4" for phosphate). The outer circle indicates the most similar or dissimilar model. The color scale in the inner and middle circles represents the dissimilarity intensity, while the outer circle's color identifies the most similar or dissimilar model

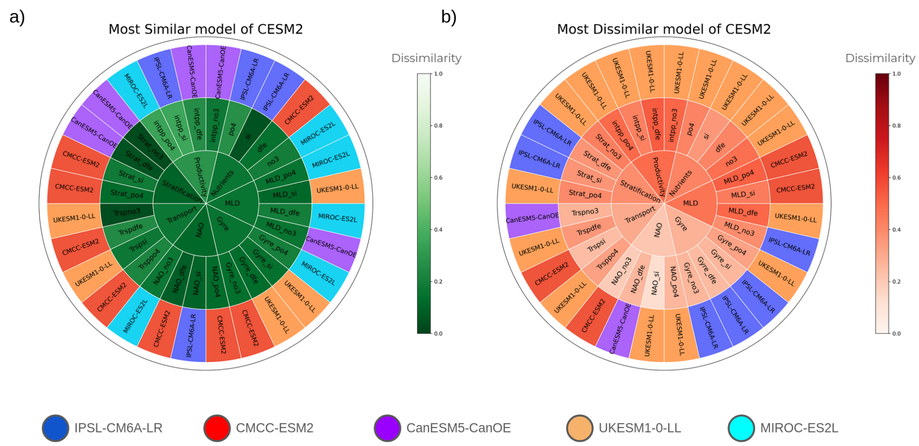

Figure S5: Same as S4 but for CESM2.

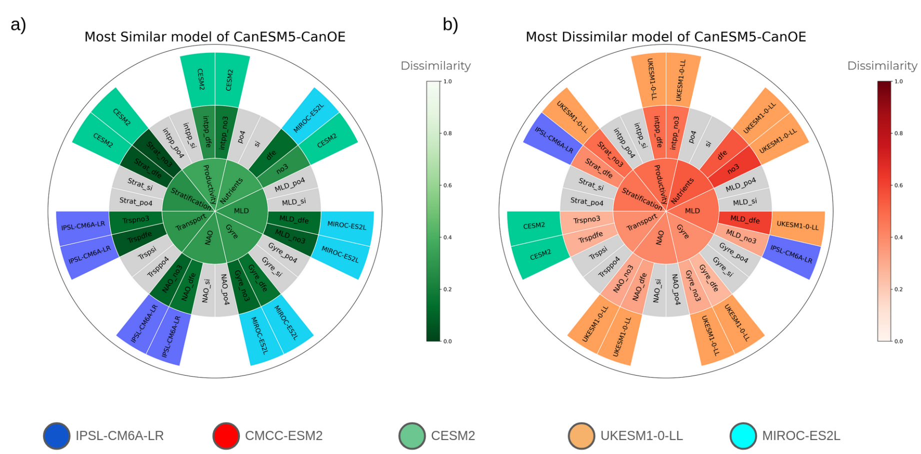

Figure S6: Same as S4 but for CanESM5-CanOE.

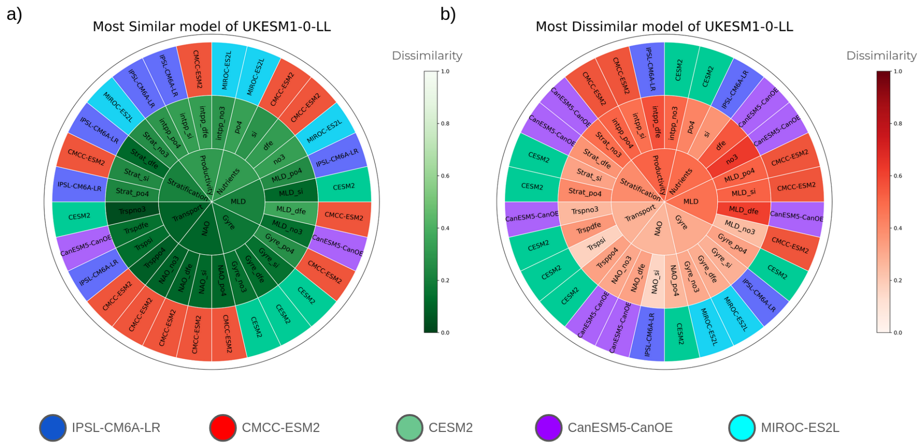

Figure S7: Same as S4 but for UKESM1-0-LL.

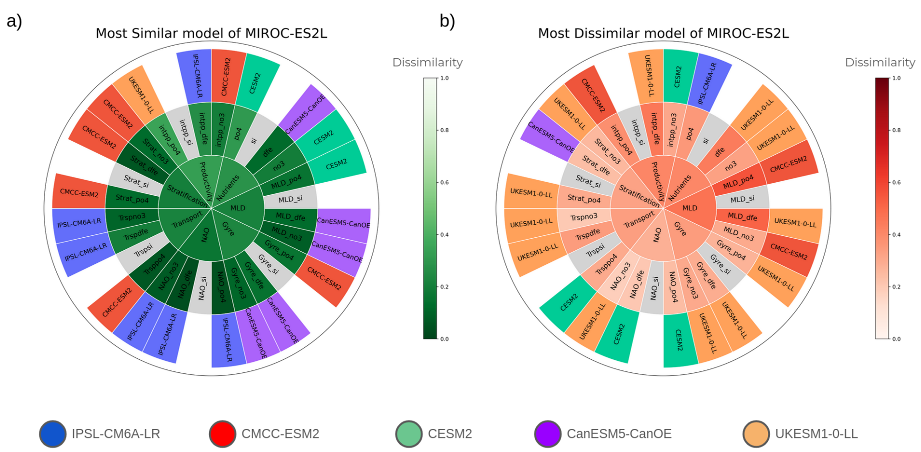

Figure S8: Same as S4 but for MIROC-ES2L.

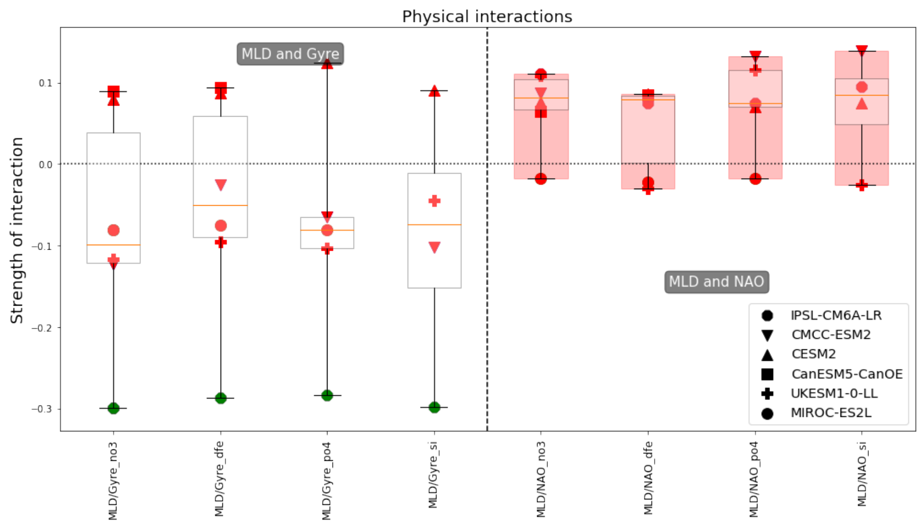

Figure S9: Additional physical interactions: Strength of links for each model with median and quartile values (boxplot). Each model is represented with a different marker and the color of the marker shows the significance of the link according to PCMCI+ (green for significant and red for not significant). Boxplots highlighted in red indicate model agreement.

References

Aumont, O., Éthé, C., Tagliabue, A., Bopp, L., and Gehlen, M.: PISCES-v2: an ocean biogeochemical model for carbon and ecosystem studies, Geoscientific Model Development Discussions, 8, 1375–1509, 2015.

Christian, J. R., Denman, K. L., Hayashida, H., Holdsworth, A. M., Lee, W. G., Riche, O. G., Shao, A. E., Steiner, N., and Swart, N. C.: Ocean biogeochemistry in the canadian earth system model version 5.0. 3: CanESM5 and CanESM5-CanOE, Geoscientific Model Development Discussions, 2021, 1–68, 2021.

Hajima, T., Watanabe, M., Yamamoto, A., Tatebe, H., Noguchi, M. A., Abe, M., Ohgaito, R., Ito, A., Yamazaki, D., Okajima, H., et al.: Development of the MIROC-ES2L Earth system model and the evaluation of biogeochemical processes and feedbacks, Geoscientific Model Development, 13, 2197–2244, 2020.

Long, M. C., Moore, J. K., Lindsay, K., Levy, M., Doney, S. C., Luo, J. Y., Krumhardt, K. M., Letscher, R. T., Grover, M., and Sylvester, Z. T.: Simulations with the marine biogeochemistry library (MARBL), Journal of Advances in Modeling Earth Systems, 13, e2021MS002 647, 2021.

Lovato, T. and Butenschön, M.: Coupling BFM with ocean models, 2020.

Lovato, T., Peano, D., Butenschön, M., Materia, S., Iovino, D., Scoccimarro, E., Fogli, P., Cherchi, A., Bellucci, A., Gualdi, S., et al.: CMIP6 simulations with the CMCC Earth system model (CMCC-ESM2), Journal of Advances in Modeling Earth Systems, 14, e2021MS002 814, 2022.

Séférian, R., Berthet, S., Yool, A., Palmiéri, J., Bopp, L., Tagliabue, A., Kwiatkowski, L., Aumont, O., Christian, J., Dunne, J., et al.: Tracking improvement in simulated marine biogeochemistry between CMIP5 and CMIP6, Current Climate Change Reports, 6, 95–119, 2020.

Vichi, M., Lovato, T., Lazzari, P., Cossarini, G., Gutierrez Mlot, E., Mattia, G., Masina, S., McKiver, W., Pinardi, N., Solidoro, C., et al.: The biogeochemical flux model (BFM): Equation description and user manual, BFM version, 5, 104, 2015.

Yool, A., Popova, E. E., and Anderson, T. R.: MEDUSA-2.0: an intermediate complexity biogeochemical model of the marine carbon cycle for climate change and ocean acidification studies, Geoscientific Model Development, 6, 1767–1811, 2013.